Long-term optical photometric monitoring of the quasar SDSS J153259.96−003944.1

C. S. Stalin[1,2] and R. Srianand[1]

[1] *IUCAA, Post Bag 4, Ganeshkhind, Pune 411 007, India*
[2] *Aryabhatta Research Institute of Observational Sciences (ARIES), Manora Peak, Nainital 263 129, India*

ABSTRACT

We report optical Cousins R and I band monitoring observations of the high redshift (z = 4.67) QSO SDSS J153259.96−003944.1 that does not show detectable emission lines in its optical spectrum. We show this object varies with a maximum amplitude of ∼0.4 mag during a year and three months of monitoring. Combined with two other epochs of photometric data available in the literature, we show the object has gradually faded by ∼0.9 mag during the period June 1998 − April 2001. A linear least squares fit to all available observations gives a slope of ∼0.35 mag/yr which translates to ∼1.9 mag/yr in the rest frame of the quasar. Such a variability is higher than that typically seen in QSOs but consistent with that of BL Lacs, suggesting that the optical continuum is Doppler boosted. Alternatively, within photometric errors, the observed lightcurve is also consistent with the object going through a microlensing event. Photoionization model calculations show the mass of the Broad Line Region to be few tens of $M_\odot$ similar to that of low luminosity Seyfert galaxies, but ∼2 orders of magnitude less than that of luminous quasars. Further frequent photometric/spectroscopic monitoring is needed to support or refute the different alternatives discussed here on the nature of SDSS J153259.96−003944.1.

Key words: quasars: general – quasars: individual: SDSS J153259.96−003944.1

1 INTRODUCTION

The diverse observational characteristics of Active Galactic Nuclei (AGN) have been reconciled in an unification scheme (Antonucci 1993; Urry & Padovani 1995). The basic idea is that all the AGNs have broad and narrow line emitting regions (BLR and NLR respectively) and an obscuring torus. Most of the diversity in the observed properties is caused by differences in our viewing angles to the torus axis. It has also been found that some of the physical parameters of AGNs show statistically significant correlations. For example, tight relationships exist between: (i) the radius of the BLR and the continuum luminosity (Corbett et al. 2003) and (ii) the black hole mass and the velocity dispersion of the host galaxy (Onken et al. 2004 and references therein). With the advent of new very large surveys, some objects that appear to depart from this standard AGN picture are beginning to emerge. Understanding these observations are important to get a clearer picture of AGN formation and evolution.

Several AGNs were recently found to have peculiar emission line characteristics. In the Sloan Digital Sky Survey (SDSS), a few high redshift quasars have been discovered without emission lines (Anderson et al. 2001;

Hall et al. 2004). Among them the z = 4.67 quasar SDSS J153259.96−003944.1 (hereafter referred to as SDSS J1533−00) first reported by Fan et al. (1999) is the object of interest in the present study. The optical spectrum of this quasar is featureless redward of the Lyα forest region; blueward of ∼6800 Å, the spectrum has features due to Lyα absorption at z = 4.52. Near-IR observations confirm the presence of a point source and an extended nebulosity in SDSS J1533−00 (see Hutchings 2003). Another object (2QZ J215454.3−305654) with similar characteristics is also reported by Londish et al. (2004).

The weak (or vanishing) emission line spectrum seen in SDSS J1533−00 is typical of BL Lac objects, where the lines are presumably swamped by the beamed and boosted continuum (Urry & Padovani 1995). BL Lac objects are characterized by strong radio and X-ray emission, optical variability and strong (and variable) optical polarization due to synchrotron radiation from a relativistic jet. Apart from the featureless spectrum, SDSS J1533−00 does not possess these other characteristic properties of BL Lac objects. It was not detected in deep radio observations (3σ upper limit of 60 μJy) and was not found to be optically polarized (with a 3σ upper limit of 4%; Fan et al. 1999). It was found to be

Table 1. Log of observations and the results of photometry. Here, QSO−A, QSO−B and A−B refer to the differential instrumental magnitudes respectively between the quasar and the comparison stars A and B, and between the comparison stars themselves

Date	λ	Exp. Time (sec)	QSO−A (mag)	QSO−B (mag)	A−B (mag)
17.01.00	R	1200	1.74 ± 0.06	2.93 ± 0.05	1.19 ± 0.02
	I	1800	0.94 ± 0.05	2.01 ± 0.05	1.07 ± 0.02
28.03.00	R	1800	1.92 ± 0.06	3.12 ± 0.06	1.20 ± 0.02
	I	1800	1.27 ± 0.05	2.31 ± 0.04	1.04 ± 0.03
30.03.00	R	1800	1.79 ± 0.06	2.99 ± 0.05	1.20 ± 0.01
	I	1800	1.24 ± 0.05	2.29 ± 0.05	1.05 ± 0.02
09.04.00	R	1800	1.81 ± 0.05	3.00 ± 0.05	1.19 ± 0.01
	I	1800	1.25 ± 0.06	2.34 ± 0.05	1.09 ± 0.02
01.05.00	R	1800	1.82 ± 0.05	2.98 ± 0.05	1.17 ± 0.02
	I	1800	1.24 ± 0.08	2.32 ± 0.07	1.08 ± 0.02
21.01.01	R	1200	1.97 ± 0.06	3.13 ± 0.06	1.16 ± 0.02
	I	1200	1.36 ± 0.07	2.35 ± 0.07	0.99 ± 0.02
26.01.01	R	900	2.10 ± 0.09	3.27 ± 0.09	1.18 ± 0.02
	I	900	1.24 ± 0.08	2.25 ± 0.08	1.01 ± 0.04
19.02.01	R	1800	1.99 ± 0.04	3.20 ± 0.05	1.21 ± 0.03
	I	1800	1.43 ± 0.04	2.46 ± 0.05	1.03 ± 0.03
25.03.01	R	300	2.05 ± 0.11	3.21 ± 0.11	1.16 ± 0.02
	I	300	1.32 ± 0.07	2.33 ± 0.07	1.02 ± 0.03
23.04.01	R	1200	2.08 ± 0.05	3.25 ± 0.05	1.17 ± 0.02
	I	1200	1.42 ± 0.05	2.44 ± 0.05	1.02 ± 0.02

an extremely weak X-ray source and was not detected in pointed Chandra observations (Vignali et al. 2001).

The absence of strong emission lines in the case of SDSS J1533−00 can be due to one of the following reasons: (i) the optical continuum being Doppler boosted as in the case of BL Lacs; (ii) the optical continuum being amplified due to a gravitational microlensing event by a star in an intervening galaxy; and (iii) absence of line emitting gas in the vicinity of the central UV continuum source. As frequent photometry of the source can confirm or reject the first two possibilities we have carried out photometric monitoring observations. In section 2 we outline the observational program, data reduction procedure and the results of the photometric monitoring. Section 3 discusses the nature of the source. Finally, our conclusions are given in Section 4. The cosmological model we consider in our study is $\Omega_m = 0.3$, $\Omega_\Lambda = 0.7$ and $H_0 = 70$ km s^{-1} Mpc^{-1}.

2 OPTICAL OBSERVATIONS AND ANALYSIS

2.1 Photometry

Optical photometric observations in Cousins R and I band were carried out on 10 nights between January 2000 and April 2001 using the 104 cm Sampurnanand telescope of the Aryabhatta Research Institute of Observational Sciences (ARIES), Nainital. This is an RC system with a f/13 beam (Sagar 1999). The detector used was a cryogenically cooled 2048×2048 CCD mounted at the cassegrain focus. Each pixel of the CCD corresponds to 0.37 (arcsec)^2 and the entire CCD covers $13' \times 13'$ on the sky. Observations were done in 2×2 binned mode to improve S/N. Typical seeing was $\sim 2''$ during most of our observations.
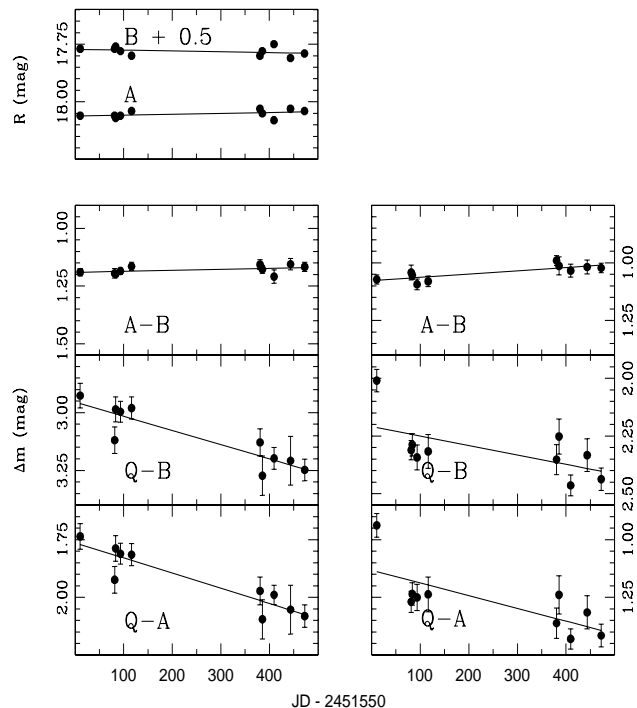

Figure 1. Differential light curves (DLCs) of the quasar SDSS J1533−00 with respect to two stars A (RA(2000) = 15:33:07.310; Dec(2000) = −00:39:04.0) and B (RA(2000) = 15:33:04.110; Dec(2000) = −00:40:49.00). The top most panel gives the standard R magnitudes of stars A and B. The other panels give the DLCs of the pair of comparison stars and between quasar and the comparison stars as indicated within the panels. The left and right panels refer to R and I bands respectively. The solid lines are the linear least squares fits to the data.

Initial processing of the images (bias subtraction, flat fielding and cosmic ray removal) were done using IRAF[1] routines, whereas PSF fitting photometry was carried out using the routines in MIDAS[2]. To look for variability, differential light curves (DLCs) of the quasar were generated with respect to stars A and B situated on the observed frames. Typical error in our photometry is around 0.03 mag for the reference stars and between 0.03 and 0.1 mag for the quasar. The log of observations and the results of the photometry are given in Table 1. The DLCs in R and I filters with respect to stars A (RA(2000) = 15:33:07.310; Dec(2000) = −00:39:04.0) and B (RA(2000) = 15:33:04.110; Dec(2000) = −00:40:49.00) are shown in Fig. 1. From Fig. 1, it appears that the quasar shows a gradual fading during the period of our observations in both R and I bands, though of course more complex behavior cannot be excluded. In particular, as we have gaps in our lightcurve, any non-linear fluctuations

[1] The Image Reduction and Analysis Facility (IRAF) is distributed by the National Astronomy Observatories, which is operated by the Association of Universities for Research in Astronomy Inc. (AURA) under cooperative agreement with the National Science Foundation

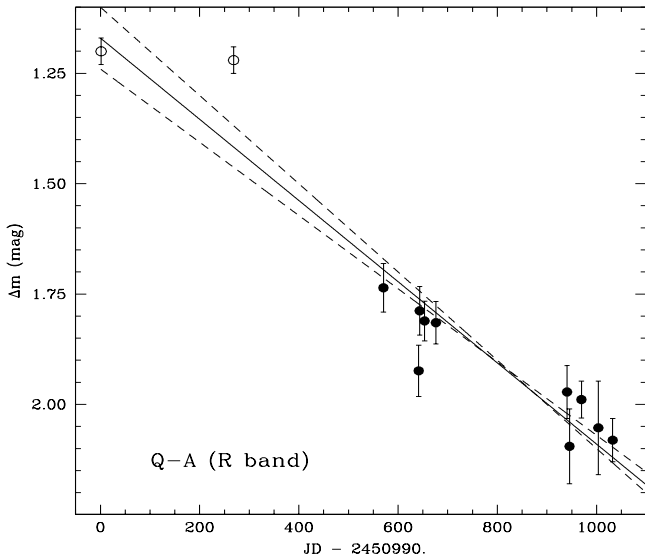[2] Munich Image Data Analysis Systems; trademark of the European Southern Observatory (ESO)

Figure 2. Differential R band light curve of the quasar SDSS J1533−00 with respect to star A (RA(2000) = 15:33:07.310; Dec(2000) = −00:39:04.0) including the observations of Fan et al. (1999) (shown as open circles). Continuous and dotted lines give respectively the linear least squares fit and 1σ error to the data.

(such as flares) cannot be ruled out. Linear least squares fits to the QSO DLCs in both R and I bands give a similar slopes of ~0.20 mag/year. However, the QSO DLCs in I band show large scatter compared to the R band data. This is due to the worse quality of the I band data due to problems in flat fielding. Also, since the R band is near the maximum of the response curve of the CCD, we consider only the R band data in any further analysis. The amplitude of variability was calculated using $A_{max} = \sqrt{(D_{max} - D_{min})^2 - 2\sigma^2}$, where D_{max} (D_{min}) are the maximum (minimum) in the quasar DLC and σ the average error in the corresponding DLC (Romero et al. 1999). The object was found to show a peak to peak amplitude of variability (A_{max}) of about 0.34 mag between January 2000 and April 2001.

SDSS J1533−00 was also observed for two epochs (27 June 1998 and 21 March 1999) by the SDSS team (Fan et al. 1999). No clear variation is observed between these two epochs. Converting their i^* magnitudes using equations (1) and (2) given by Fukugita et al. (1996) and the zero point given by Bessel (1979), the R band magnitudes are estimated as 19.66 and 19.68 on 27 June 1998 and 21 March 1999 respectively. In order to compare these quasar magnitudes to its magnitude during the epoch of our observations, we converted the quasar's instrumental magnitudes during our observations to apparent R magnitudes by the technique of differential photometry using Star A at the position (RA(2000) = 15:33:07.310; Dec(2000) = −00:39:04.0 and whose R band magnitude of 18.46 mag is taken from USNO–B; Monet et al. 2003) available on the quasar CCD frame. The apparent R magnitude of the quasar thus calculated during our period of observations range from 20.20 to 20.56 mag. Thus, combining our observations with those reported by the SDSS team, we find that the quasar has

faded by ~0.9 mag over a period of about 3 years from June 1998 to April 2001. Using a simple least squares fit to all the available data we get (see Fig. 2),

$$\Delta m(mag) = (1.17 \pm 0.07) + (0.34 \pm 0.03) \times t(yr). \qquad (1)$$

Here, Δm is the differential magnitude of the quasar with respect to the reference star A and t is the time in the observer's frame.

2.2 Spectroscopy

We use the optical spectrum of SDSS J1533−00, obtained by Fan et al. (1999) with the Keck II telescope using the Low Resolution Imaging Spectrograph, to obtain the optical continuum spectral index, α_0 (defined through, $S_\nu \propto \nu^{\alpha_0}$), and an upper limit of the Lyα emission line flux. The observed spectrum is well fitted with the existence of Lyα absorption system at $z_{abs} = 4.58$ with N(H I) = 1.1 $\times10^{21}$ cm^{-2}, Lyα emission line with a FWHM of 105 Å (or a velocity width of 4630 km/s) at an emission redshift of $z_{em} = 4.67$ and $\alpha_0 = -0.8$. N(H I) in the absorbing gas cloud is obtained by self-consistently fitting Lyα, Lyβ and Lyγ lines. The fit to the spectrum is shown in Fig. 3. Inclusion of Lyα emission in the fitting improves the fitting of the Lyα absorption line. However, as noticed by Fan et al. (1999) the higher Lyman series lines do not show complete absorption suggesting the gas producing the absorption cannot be a strong damped Lyα system. Thus our fits will over predict the N(H I) in the absorbing gas and the derived upper limit of the Lyα emission line flux.

The estimated flux of the fitted Lyα emission line is $\leqslant 1.06\times10^{-15}$ erg cm^{-2} s^{-1}. This corresponds to an emitted luminosity of $\leqslant 2.2 \times 10^{44}$ erg s^{-1}. Using the fitted continuum and emission line flux we get an upper limit ($\simeq 9.9$ Å) on the rest frame Lyα emission line equivalent width.

2.2.1 Excess continuum flux

As discussed before, the lack of emission lines in the spectrum of SDSS J1533−00 can be due to the continuum emission being enhanced either by Doppler boosting of the relativistic optical jet emission or by gravitational lensing of the continuum but not the line emitting BLR. From the observed spectrum we obtain an estimate of the enhancement needed in the optical continuum so that the emission lines appear weak. This is done by calculating the equivalent width of Lyα emission line from the observed spectrum of SDSS J1533−00 and comparing it with the typical Lyα emission line equivalent width observed in the composite spectrum of quasars (Francis et al. 1991). The equivalent width (EW) is defined as

$$W_{obs} = \frac{F_{line}}{\mu F_{cont}} \qquad (2)$$

where μ is the magnification. The rest frame W_{obs} is 9.9 Å. When compared with the typical EW of about 80 Å(Francis et al. 1991) observed in quasars, this gives a magnification of $\geqslant 8$. Thus roughly an order of magnitude amplification in the continuum flux is needed to explain the observed weakness of the Lyα emission line if it is not due to a lack of emitting gas.
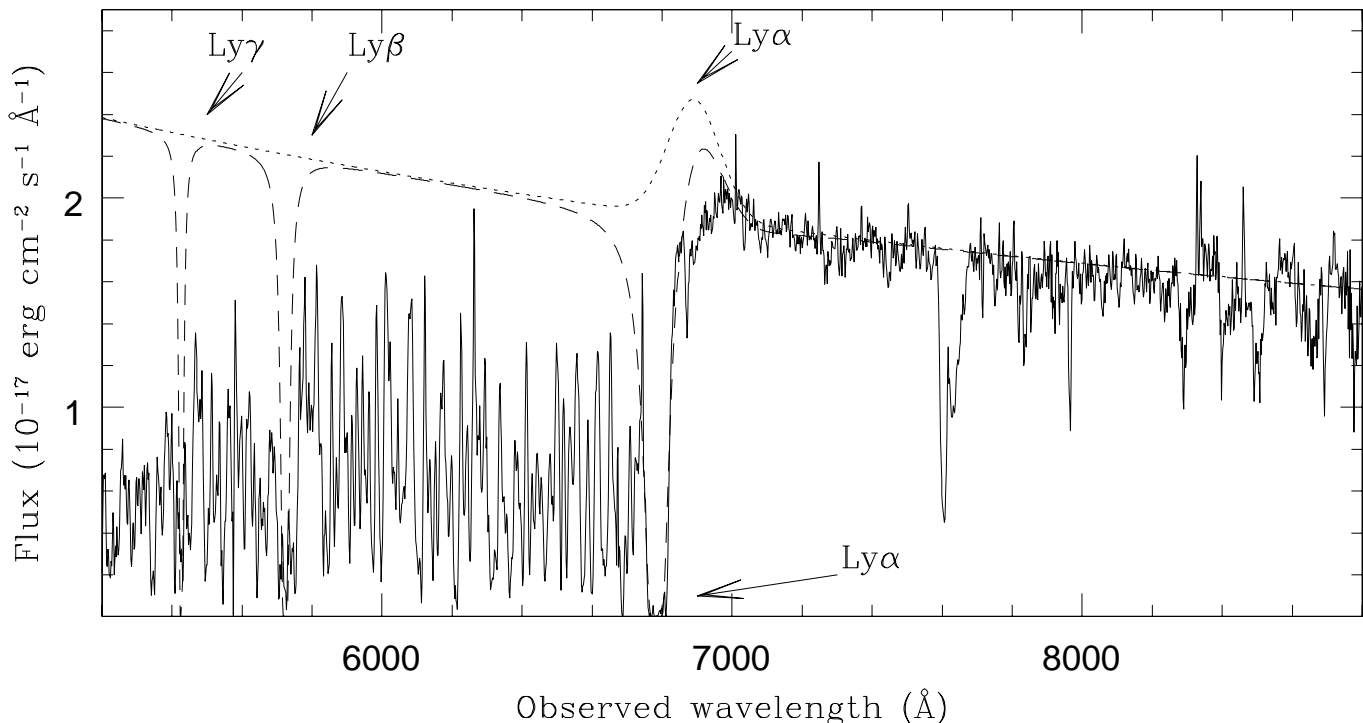
Figure 3. The observed optical spectrum of the quasar using the LRIS spectrograph on Keck II (solid line) along with the fitted absorption and emission lines. The dotted line shows the modeled spectrum containing only the Lyα emission line whereas the dashed line shows the modeled spectrum containing both Lyα emission and absorption lines of Lyα, Lyβ and Lyγ.

3 DISCUSSION

3.1 Nature of optical variability of SDSS J1533−00

The absence of strong emission lines in the spectrum of SDSS J1533−00 is similar to that of BL Lacs. It is also believed that the lack of emission lines in BL Lacs is due to the continuum being Doppler boosted. One of the defining characteristics of BL Lacs is that they show large amplitude flux variability over the entire electro-magnetic spectrum. Here, we discuss the observed variability properties of SDSS J1533−00 and the known properties of the different kinds of AGNs derived based on long term optical monitoring to understand the nature of SDSS J1533−00. The R band observations correspond to $\sim$1230 Å in the QSO rest-frame. A linear least squares fitting to our observations (see Eq. 1) combined with two other epochs of observations of the SDSS team, gives a rate of change of $\sim$0.35 mag/yr in R band in the observed frame. This when transformed to the rest frame of the quasar (taking into account the effects of time dilation; $t_{rest} = t_{obs}(1+ z)$) gives a rate of decline in the R band magnitude of $\sim$1.9 mag/yr. This rate of decline is an average, in reality the decline could be more dramatic if there had been a flare in the intervening period.

Comparing SDSS and POSS measurements on a large sample of SDSS quasars, de Vries et al. (2003) have reported that the long term quasar variability is consistent with a decaying intrinsic light-curve of the form, $1.1 \times \exp(-t(yr)/2)$. Similar variability time-scales ($\sim$1 year) and amplitudes

($\sim$0.16 mag) have also been found by Trevese et al. (1994) from a 15 year monitoring of 35 quasars between $0.6 < z < 3.1$. Giveon et al. (1999) have reported an average rate of change in the intrinsic B band magnitude of 0.28 mag/year using 7 years of monitoring data on 42 low-luminosity PG quasars sample with $z < 0.4$. For the same data, Cid Fernandes et al. (2000), using structure function analysis, report a variability amplitude and time-scale of 0.18 mag and 1.8 years respectively. Recently, using large database of variability on SDSS quasars, Ivezić et al. (2004) report a variability amplitude and time-scale of 0.32 mag and 1 year, respectively. Thus, it appears that the normal population of QSOs seem to show an intrinsic rate of change of $\leqslant 0.5$ mag/yr. In contrast, from the published lightcurves of blazars monitored over a 18 year time baseline (Webb et al. 1988), considering the long term trends, we notice that blazars on an average show a larger rate of variability ($\geqslant 1$ mag/yr).

From the above discussions, it is clear that the observed R band variability of 1.9 mag/yr shown by SDSS J1533−00 is larger than that seen in typical QSO population. As SDSS J1533−00 is highly luminous ($M_{1450\text{\AA}} = -26.6$ mag), X-ray and radio quiet and at high redshift, based on the existing correlations (de Vries et al. 2004; Vanden Berk et al. 2004; Cid Fernandes et al. 1996; Cristiani et al. 1996; Giveon et al. 1999), we expect it to show a lower rate of change of magnitude. However, the observed high rate of variability is consistent with that seen in BL Lac objects. Thus our observations are consistent with SDSS J1533−00 being a low luminosity AGN (with intrinsically weak emission lines)

with its continuum being boosted by relativistic beaming. However, the continuum emission mechanism in the jet of this object needs to be very different from typical BL Lac objects, since its broad-band properties are so discordant.

Although the sparse long-term variability nature of SDSS J1533−00 is similar to BL Lacs, intra-night monitoring observations too are needed to confirm the presence of relativistic optical continuum emitting jet in SDSS J1533−00. This is due to the fact that the observed large amplitude and frequent variability of BL Lacs on intra-night timescales (Stalin et al. 2004; Gopal-Krishna et al. 2003) is now widely believed to be due to the inhomogeneities in the outflowing relativistic jet. Such a study is planned in the coming observing season.

3.2 Is variability due to microlensing?

In this section, we explore the possibility that the observed decline in the light curve of SDSS J1533−00 is due to microlensing of the continuum source by an intervening object. Such a model was proposed by Ostriker & Vietri (1985) to explain BL Lac objects (see also Gopal-Krishna and Subramanian 1991, for a relativistically moving source). Microlensing in the intervening galaxy is believed to be the cause of abnormal emission line ratios seen among different components in the multiply imaged systems such as Q2237+030 (Huchra et al. 1985), APM 08279+5255 (Lewis et al. 2002) and SDSS J1004+4112 (Richards et al. 2004). As the QSO is not multiply imaged, the line of sight to the QSO most probably samples the outer region of the intervening galaxy. However, we note that the required magnification (i.e., $\geqslant 10$) of the continuum for the emission lines to be invisible in SDSS J1533−00 is much higher than that required in the case of multiply imaged systems discussed above (i.e., ~ 2).

For the continuum source (and not the broad line emitting region) to be magnified significantly due to microlensing, the microlensing length scale, i.e., the Einstein radius, should be larger than the projected radius of the continuum emitting region ($\leqslant 10^{14}$ cm) and smaller than the radius of the BLR (few 10^{17} cm). The Einstein radius (R_E) is defined as

$$R_E = \sqrt{\frac{4GM}{c^2} \frac{D_{ls}}{D_l D_s}} \qquad (3)$$

where D_l, D_{ls} and D_s are the lens, source-lens and source angular diameter distances, respectively, and M is the mass of the lens. For a lens mid-way between the source and the observer (which corresponds to a lens redshift of 0.678), R_E is ~ 0.01 pc for 1 $M_\odot$ lens. Such a lens will satisfy the requirements for microlensing described above. We notice that to get the required high magnification the impact parameter has to be less than 1.5×10^{15} cm at the lens plane. The rate of change of magnification will depend upon the velocity of the star for a given impact parameter.

We obtain the expected light curve in the observer's frame assuming the velocity of the lens to be 200 km s^{-1} in the lens plane for different impact parameters (using equation 20 of Refsdal 1964). The results are shown in Fig. 4 where we plot the log of magnification as a function of time. As we do not know the intrinsic flux and the epoch
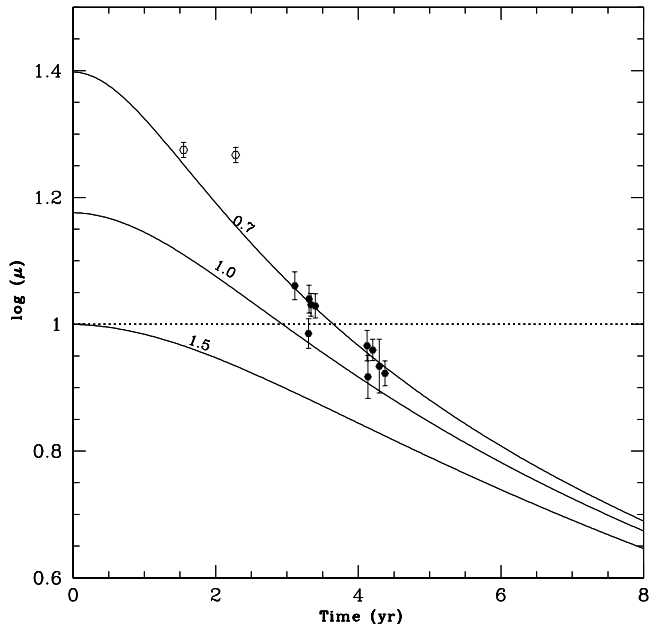

Figure 4. Simulated microlensing lightcurves (log of magnification versus time) for three impact parameters. Our observations (filled circles) as well as those of Fan et al. (1999) (open circles) are overplotted on the modeled lensing lightcurves. The impact parameter in units of 10^{15} cm is given against each curve. The dotted horizontal line indicates a magnification of 10.

at which SDSS J1533−00 was at its maximum magnification, we shifted the observed points to match the predicted curve with similar slope. From Fig. 4 it is clear that the sparsely sampled observed light curve can match the predicted lensing curve for an impact parameter of $\sim 7 \times 10^{14}$ cm for an assumed solar mass lens moving at 200 km s^{-1}. The required impact parameter will be slightly higher if we assume the velocity of the lensing star to be higher than 200 km s^{-1}. This simple exercise demonstrates that microlensing is a viable option in this case. Interestingly, the QSO is found to be surrounded by excess density of galaxies, with the closest companion galaxy at a separation of only $\sim 3.5''$ from the QSO (Hutchings 2003). We need closely sampled multi-band light curves to confirm or refute this microlensing scenario. Also, if microlensing is the correct option, then we now expect the Lyα emission line to become more clearly visible in the spectrum of the QSO as the enhanced continuum continues to decline. Further photometric and spectroscopic observations should thus constrain the microlensing hypothesis.

3.3 How much gas is there in the BLR?

The upper limit we derive on the Lyα line flux (see Sect. 2.2) can be used to obtain a limit on the mass of the line emitting gas in the BLR. If BLR gas emits very efficiently then the mass of the BLR (M_{BLR}) is given by

$$M_{BLR} = 5.1(10^{11}/n_e)(L_{\text{Ly}\alpha}/10^{45}) \ M_\odot \qquad (4)$$

For the upper limit of Lyα luminosity of SDSS 1533−00, we get $M_{BLR} \leqslant 1.1 \ M_\odot$ for $n_e = 10^{11}$ cm^{-3}. As pointed out by

Table 2. Results of photoionization model computations. Here, N(HI) = total hydrogen column density, n_H = hydrogen density, R_{BLR} = radius of the BLR, log U = logarithm of ionization parameter, L(Lyα) = luminosity of L(Lyα) emission line, N_c = number of Lyα emitting clouds and M_{BLR} = mass of the BLR

N(HI) (cm^{-2})	n_H (cm^{-3})	R_{BLR} (pc)	log U	L(Lyα) (erg s^{-1})	N_c	M_{BLR} ($M_\odot$)
10^{20}	10^9	0.8 (0.17)	-0.29 (0.07)	1.21×10^{28} (1.42×10^{28})	1.9×10^{16} (1.6×10^{16})	8.16 (6.96)
	10^{12}	0.8 (0.17)	-3.29 (-2.93)	2.09×10^{24} (2.69×10^{24})	1.1×10^{20} (8.4×10^{19})	0.05 (00.04)
10^{21}	10^9	0.8 (0.17)	-0.29 (0.07)	8.36×10^{30} (8.07×10^{30})	2.7×10^{13} (2.8×10^{13})	11.83 (12.25)
	10^{12}	0.8 (0.17)	-3.29 (-2.93)	2.91×10^{26} (6.26×10^{26})	7.7×10^{17} (3.6×10^{17})	0.34 (00.16)
10^{22}	10^9	0.8 (0.17)	-0.29 (0.07)	7.76×10^{33} (7.00×10^{33})	2.9×10^{10} (3.2×10^{10})	12.75 (14.13)
	10^{12}	0.8 (0.17)	-3.29 (-2.93)	2.92×10^{28} (6.30×10^{28})	7.7×10^{15} (3.6×10^{15})	3.38 (01.57)
10^{23}	10^9	0.8 (0.17)	-0.29 (0.07)	6.04×10^{36} (6.21×10^{36})	3.7×10^{07} (3.6×10^{07})	16.38 (15.92)
	10^{12}	0.8 (0.17)	-3.29 (-2.93)	2.92×10^{30} (6.30×10^{30})	7.7×10^{13} (3.6×10^{13})	33.83 (15.70)

Baldwin et al. (2003) the mass estimated using the above equation will be the minimum mass in the BLR. We obtain a realistic upper limit to M_{BLR} using the photoionization code CLOUDY (Ferland et al. 1998).

The ionization state of the line emitting gas is quantified using a dimensionless ionization parameter, U. This is defined as,

$$U = \frac{L_{912}}{4\pi R_{BLR}^2 h\nu c n} \quad (5)$$

where n, L_{912} and R_{BLR} are, respectively, the number density of the gas particles, the Lyman continuum luminosity, and the radius of the BLR around the central engine. We obtain $L_{912} = 2.7 \times 10^{46}$ erg s^{-1} using the observed flux above the Lyα emission line and a spectral index, $\alpha_o = -0.8$ (see Sect. 2.2). For a standard AGN, R_{BLR} can be estimated from the rest-frame luminosity at 5100 Å(i.e., L_{5100}) using

$$R_{BLR} = 27.4 \left(\frac{L_{5100}}{10^{44} \text{ergs}^{-1}} \right)^{0.68} \text{ light days}, \quad (6)$$

(see Corbett et al. 2003 and references therein). The above relationship is established using reverberation mapping studies. Assuming such a relationship holds good even for SDSS J1533−00, we estimate the radius of the BLR to be 0.8 pc. Thus we have a constraint on U for an assumed value of n. For example, when we consider $n = 10^9$ cm^{-3} the consistent value of log$U$ is -0.29.

We then estimated the Lyα emission line luminosity from a single cloud ($L(\text{Ly}\alpha)^{cal}$) for a given n, U, total hydrogen column density N(HI) and ionizing spectrum of the QSO using the photoionization code CLOUDY (Ferland et al. 1998). This together with the observed upper limit on the Lyα emission line flux ($F(Ly\alpha)^{obs}$) is used to get the number of BLR clouds,

$$N_c = \frac{4\pi d_l^2 F(\text{Ly}\alpha)^{obs}}{L(\text{Ly}\alpha)^{cal}}. \quad (7)$$

Here, for simplicity we assume all the BLR clouds to be identical. In addition if we assume the clouds to be spherical we can get the mass of the Lyα emitting clouds in the BLR. The total mass of the BLR contained in N_c clouds is calculated using

$$M_{BLR} = N_c \times \frac{4}{3}\pi r^3 \rho \quad (8)$$

where ρ and r are the total hydrogen mass density and radius of the cloud ($r = N(\text{HI})/2n$), respectively.

The ionizing continuum used in the model calculations is a combination of a UV bump (assumed to be a blackbody with a temperature of 10^6 K) and an X-ray power law (Georgantopoulos et al. 2004) of the form $f_\nu \propto \nu^{-2.0}$. The UV and the X-ray continuum slopes were combined using an UV to X-ray logarithmic spectral slope of $\alpha_{ox} = -2.0$. This value of α_{ox} is consistent with the upper limit derived by Vignali et al. (2003).

For this assumed incident ionizing continuum shape and solar chemical abundances, we carried out grids of photoionization model computations for various values of N(HI) and n. The chosen range in N(HI) considers BLR to range from optically thin to optically thick. The ranges of other chosen parameters are also consistent with those frequently used in BLR modeling (see Korista et al. 1997). The results of these model calculations are summarized in Table 2. It is found that the calculated values of the $Ly\alpha$ emission line luminosity are weakly dependent on the input values of α_{ox}. We also notice that changing the temperature of the UV bump from 10^5 K to 10^6 K changes the luminosity by less than a factor of 2. Assuming the observed continuum is enhanced by a factor of 10 (due to either Doppler boosting or gravitational lensing), we also carried out photoionization model computations by de-magnifying the measured continuum luminosity by a factor of 10. The results are shown within brackets in Table 2.

Clearly our model calculations are consistent with $M_{BLR} < 50\ M_\odot$ in the case of SDSS J1533−00. This is 1 to 2 orders of magnitude less than that derived for the standard high luminosity QSOs (Baldwin et al. 2003). However, the estimated upper limit is consistent with BLR masses computed for low luminosity Seyfert galaxies (see Peterson 2004).

4 CONCLUSION

We have presented optical photometric monitoring of the peculiar quasar SDSS J1533−00 for a duration spanning about 500 days during which the object has varied by about 0.4 mag. These observations, when coupled with two other epochs of observations available in the literature, indicate that the quasar gradually faded by 0.9 magnitude during the period June 1998 to March 2001. This transforms to a variability of ∼1.9 mag/yr in the rest frame of the quasar. Such a large amplitude of variability is similar to the long

term variability nature of BL Lacs. Nevertheless, the lack of X-ray and radio emission and optical polarization suggests that the continuum emission in the jet needs to be very different from BL Lacs. Available photometric data on the source could not rule out microlensing as the cause of the variability as well as the observed lack of emission lines. Further monitoring observations are needed to constrain the microlensing scenario.

   Photoionization model calculations show the BLR mass to be consistent with low luminosity Seyferts (Peterson 2004), but ∼2 orders of magnitude lower compared to those expected for high luminosity quasars (Baldwin et al. 2003). It is also possible that SDSS J1533−00 belongs to an unknown population of highly luminous AGNs without a BLR. This would be in line with the "naked" AGNs discussed by Hawkins (2004). Furthermore, if the observed lack of emission lines in the discovery spectrum of SDSS J1533−00 (Fan et al. 1999) is due to the continuum being amplified either due to Doppler boosting or to gravitational lensing, then we might expect to see emission lines emerge as our observations show the quasar to be in the declining phase. Further photometric and spectroscopic observations could clarify the peculiar nature of SDSS J1533−00.

   There now exist quite a few other objects with featureless optical spectra resembling BL Lacs but which lack the significant radio and X-ray emission found in BL Lacs (Anderson et al. 2001; Hall et al. 2004; Londish et al. 2002). Whether SDSS J1533−00, along with such other objects, fit into the orientation based unification scheme, or whether they instead belong to a hitherto unrecognized population of radio-quiet BL Lacs or lineless radio-quiet quasars remains an open question.

ACKNOWLEDGEMENTS

REFERENCES

Anderson S. F., et al 2001, AJ, 122, 503

Antonucci R. 1993, ARA&A, 31, 473

Baldwin J.A., Ferland G.J., Korista K.T., Hamann F., Dietrich M., 2003, ApJ, 582, 590

Bessel, M. S. 1979, PASP, 91, 589

Cid Fernandes R., Sodre Jr. L., Vieira Da Silva, Jr., 2000, ApJ, 544, 123

Cid Fernandes R., Aretxaga I., Terlevich R., 1996, MNRAS, 282, 1191

Corbett, E.A., et al. 2003, MNRAS, 343, 705

Cristiani S., Trentini S., La Franca F., Aretxaga I., Andreani P., Vio R., Gemmo A., 1996, A&A, 306, 395

De Vries W.H., Becker R.H., White R.L., Loomis C., 2004 (astro-ph/0411348)

De Vries W.H., Becker R.H., White R.L., 2003, AJ, 136, 1217

Fan, X., et al. 1999, ApJL, 526, L57

Ferland G.J., Korista K.T., Verner D.A., Ferguson J.W., Kingdon J.B., Verner E.M., 1998, PASP, 110, 761

Francis P.J., Hewett P.C., Foltz C.B., Chaffee F.H., Weymann R.J., Morris S.L., 1991, ApJ, 373, 465

Fukugita M., Ichikawa T., Gunn J. E., Doi M., Shimasaku K., Schneider D. P. 1996, AJ, 111, 1748

Georgantopoulos I., Georgakakis A., Akylas A., Stewart G. C., Giannakis O., Shanks T., Kitsionas S. 2004, MNRAS, 352, 91

Giveon U., Maoz D., Kaspi S., Netzer H., Smith P.S., 1999, MNRAS, 306, 637

Gopal-Krishna, Subramonian, K. 1991, Nature, 349, 766

Gopal-Krishna, Stalin C.S., Sagar R., Wiita P.J., 2003, ApJL, 586, 25

Hall P. B. et al. 2004, AJ, 128, 534

Hawkins, M. R. S. 2004, A&A, 424, 519

Huchra J., Gorenstein M., Kent S., Shapiro I., Smith G., Horine E., Perley R., 1985, AJ, 90, 691

Hutchings, J. B. 2003, AJ, 125, 1053

Ivezic Z., et al. 2004 in Interplay among black holes, stars and ISM in galactic Nuclei (eds) Th. Storchi Bergmann, L.C. Ho & H.R. Schmidt

Korista K., Baldwin J., Ferland G., Verner D., 1997, ApJS, 108, 401

Lewis G.F., Ibata R.A., Ellison S.L., Aracil B., Petitjean P., Pettini M., Srianand R., 2002, MNRAS, 334, 7

Londish D., Heidt J., Boyle B. J., Croom S. M., Kedziora-Chudczer L. 2004, MNRAS, 352, 903

Londish D., et al 2002, MNRAS, 334, 941

Monet D.G., et al. 2003, AJ, 125, 984

Onken C.A., Ferrarese L., Merritt D., Peterson B.M., Pogge R., Vestergaard M., Wandel A., 2004, ApJ, 615, 645

Ostriker, J. P., Vietri, M. 1985, Nature, 318, 446

Peterson B.M., 2004 in Physics of Active Galactic Nuclei at all scales, eds. D. Alloin, R. Johnson & P. Lira, Lecture Notes in Physics

Refsdal S., 1964, MNRAS, 128, 295

Richards G.T., et al. 2004, ApJ, 610, 679

Romero, G. E., Cellone, S. A., Combi, J. A. 1999, A&AS, 135, 477

Sagar, R., 1999, Current Science, 77, 648

Stalin C.S., Gopal-Krishna, Sagar R., Wiita P.J., 2004, JApA, 25, 1

Trevese D., Kron R.G., Majewski S.R., Bershady M.A., Koo D.C., 1994, 433, 494

Urry, C. M., Padovani, P. 1995, PASP, 107, 803

Vanden Berk D.E., et al. 2004, ApJ, 601, 692

Vignali, C., Brandt, W. N., Fan, X., Gunn, J. E., Kapsi S., Scheider D. P., Strauss M. 2001, AJ, 122, 2143

Vignali C., et al. 2003, AJ, 125, 2876

Webb J.R., Smith A.G., Leacock R.J., Fitzgibbons G.L., Gombola P.P., Shepherd D.W., 1988, AJ, 95, 374